

Synthesis of Mn₃O₄ Microflowers Anode Material for Lithium-ion Batteries with Enhanced Performance

ABSTRACT

A simple and versatile method for preparation of Mn₃O₄ microflowers associated with super-thin nanosheets is developed via a solvo-thermal approach, which are tested as a new high-capacity anode material for lithium-ion batteries. It shows better cycling performance than Mn₃O₄ nanoparticles. Research on this topic mainly sheds some light on the preparation of three-dimensional flower-like oxide hierarchical architectures with improved electrochemical performance for energy storage.

Keywords: Manganese oxide; Hierarchical architectures; Anode; Lithium-ion battery; Surfactant; Nanosheet.

1. INTRODUCTION

Rechargeable batteries with reversible and efficient electrochemical energy storage and conversion are urgent in various applications, such as portable electronic consumer devices, electric vehicles, and large-scale electricity storage in smart and intelligent grids as renewable and clean energy[1, 2]. Lithium-ion battery is one of the fascinating rechargeable batteries for high energy density coupled with a long life cycle and charge-discharge rate capability[3]. Studies have been conducted to develop low-cost, sustainable, renewable, safe, and high-energy density electrode materials for lithium-ion batteries. Considering environmental safety, researchers should prepare potential electrode materials for lithium-ion batteries through green chemistry based on simple and inexpensive procedures.

Manganese based anode materials are less toxic, abundant in natural resources[4]. Though Mn₃O₄ is isostructural with Co₃O₄, it has poor lithiation activity and electrically insulating, resulting in fast capacity decay as anode materials for lithium-ion batteries. Recently great progress has been achieved for Mn₃O₄ anode materials. The improved electrochemical properties turned true via the following methods. Mesoporous carbon, graphene, carbon nanotube and various carbon nanostructures were introduced to prepare carbon based Mn₃O₄ nano-composites. These composites showed better cycling stability and higher discharge capacity than bulk Mn₃O₄ for fast ion diffusion, good electronic conductivity, and skeleton supporting function[5-35]. People also designed various Mn₃O₄ nanostructures to improve the cycling performance of Mn₃O₄. In these Mn₃O₄ nanostructures, well-shaped nanostructure, pore, hollow structure and 3D array played an important role in the long cycling performance. Novel pongelike nanosized Mn₃O₄ exhibits a high initial reversible capacity of 869 mAhg⁻¹ and significantly enhanced first coulomb efficiency with a stabilized reversible capacity of around 800 mAhg⁻¹ after over 40 charge/discharge cycles [4]. Mn₃O₄ hollow microspheres demonstrate a good electrochemical performance, with a high reversible capacity of 646.9 mAhg⁻¹ after 240 cycles at a current density of 200 mAhg⁻¹[36]. While fluorinated Mn₃O₄ nanospheres for lithium-ion batteries show poor cycling performances[37]. 3D porous Mn₃O₄ nanosheet arrays could be directly used as a binder-free and conductive-agent-free electrode to deliver ultrahigh electrochemical performance [38]. It is reported that the 3D pores and voids between the nanosheet arrays could provide rapid ion transfer channels, as well as accommodating the volumetric changes of Mn₃O₄ during the electrochemical cycling[38]. The ultrathin Mn₃O₄ nanosheets exhibit a high reversible capacity and stronger cycling stability for high surface area[39]. The well-shaped Mn₃O₄ tetragonal bipyramids with high-energy facets show a high initial discharge capacity. In addition, the anode displays a good fast rate performance and delivers a reversible capacity of 822.3 mAhg⁻¹ (the theoretical capacity: 937 mAhg⁻¹ at a current density of 0.2 C after 50 cycles[40]. The porous Mn₃O₄ nanorods can improve electrochemical reaction kinetics and favor the formation of Mn₃O₄ [41]. Mn₃O₄ nano-octahedra has a discharge capacity of 667.9 mAhg⁻¹ after 1000 cycles at 1.0 A g⁻¹ ascribed to the lower charge transfer resistance due to the exposed highly active {011} facets, which can facilitate the conversion reaction of Mn₃O₄ and Li owing to the alternating Mn and O atom layers,

49 resulting in easy formation and decomposition of the amorphous Li₂O and the multi-electron
50 reaction[42]. The hollow Mn₃O₄ spheres deliver a highly stable cycle performance with capacity
51 retention of similar to 980 mAhg⁻¹ for over 140 cycles at 200 mA_g⁻¹ and an excellent rate
52 capability[43]. It can be seen that Mn₃O₄ with nanosheets, pore, high surface area and
53 interconnected voids are apt to show high discharge capacity and long cycling stability. The 3D
54 assembling Mn₃O₄ microflowers assembling with nanosheets are expected to show favorable
55 electrochemical performances for the presence of voids among the nanosheet arrays. There are few
56 reports on the research of Mn₃O₄ microflowers except Mn₃O₄-Fe₃O₄ and MnO- Mn₃O₄ nanoflowers.
57 Mn₃O₄-Fe₃O₄ nanoflowers are simply fabricated through one step etching Mn₅Fe₅Al₉₀ ternary alloy,
58 which exhibits higher performance as anode material for lithium ion batteries than that of pure Mn₃O₄
59 and Mn₃O₄ anodes for unique hierarchical flower-like structure and the synergistic effects between
60 Mn₃O₄ and Mn₃O₄ [44]. A hierarchically porous MnO- Mn₃O₄ nano-flowers can be fabricated by
61 dealloying Mn/Al alloys in aqueous NaOH solution in the presence of H₂O₂, and upon annealing,
62 which has a capacity of 1018, 901 and 757 mAhg⁻¹ with nearly 100% retention capacity after 100
63 cycles at 100, 200 and 500 mA_g⁻¹[45]. Mn₃O₄ nanosheets associated with nanorods can be
64 assembled to 3D flower-like Mn₃O₄ with hexadecyl trimethyl ammonium bromide (CTABr), urea and
65 MnSO₄ as reagents, while they did not tested any properties, e.g. batteries [46].

66

67 **2. MATERIAL AND METHODS / EXPERIMENTAL DETAILS / METHODOLOGY (ARIAL, 68 BOLD, 11 FONT, LEFT ALIGNED, CAPS)**

69

70 All chemicals are commercially available. The preparation was performed via a solvothermal method
71 in a DMF-water mixed solvent. In a typical procedure, 1 mmol manganese acetate tetrahydrate and
72 0.5 g hexadecyl trimethyl ammonium bromide (CTABr) were added to a 5 ml DMF- 25 ml water
73 solution and stirred at room temperature for 2 hours. After that, the mixture was transferred to a 50-ml
74 Teflon-lined stainless autoclave, sealed, kept at 200 °C for 24 hours, cooled to room temperature,
75 washed with absolute alcohol and dried at 70 °C for 12 hours (marked with DT-1). Sample DT-2 was
76 prepared without CTABr under the identical condition. While Sample DT-3 was prepared with 30 ml
77 water in the absence of CTABr.

78 The morphological characteristics of the as-synthesized materials were observed with a Hitachi S-
79 4800 field emission scanning electron microscope (SEM). X-ray diffraction (XRD) patterns were
80 recorded on a diffract meter (Co K α , Analytical, and Pert). Cyclic voltammetry (CV) experiments were
81 performed with a Chi660c electrochemical workstation at a scan rate of 1 mV S⁻¹. A Land CT2001A
82 battery tester was used to measure the electrode activities at room temperature.

83 The as-synthesized samples were tested as anode materials for lithium-ion batteries. The composite
84 of negative electrode material was consisted of the active material, a conductive material (super-pure
85 carbon) and binder polyvinylidene difluoride (PVDF) in a weight ratio of 7/2/1. The Li metal was used
86 as the counter electrode. The cells were charged and discharged between a 0.05 - 3.0 V voltage limit.
87

88 **3. RESULTS AND DISCUSSION**

89

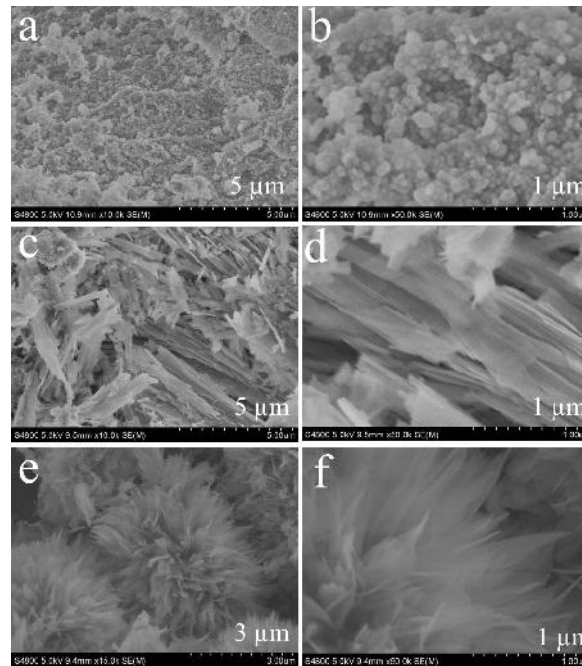
90 Three samples were obtained by adjusting synthesis parameters. Both DMF and CTABr play an
91 important role in the formation of different morphologies. When water was used as the solvent in the
92 absence of CTABr, the sample appears as monodispersed nanoparticles between 30 and 150 nm in
93 Fig. 1a,b. While DMF was added, thin microplatelets were obtained, as shown in Fig. 1c, d. The
94 length and width of microplatelets can be up to several μ m. There are also some thin nanobelts.
95 Some microflowers composed of superimposed thin and wide nanosheets were prepared with CTABr
96 in the DMF-H₂O mixed solvent in Fig. 1c, d. Certain microflower is several μ m in size.
97

98 X-ray diffraction was performed to identify the structure of the three samples. It can be seen that
99 CTABr plays an important role in the crystallization of products. The diffraction peaks of the sample
100 prepared with DMF, water and CTABr has the highest intensity than samples prepared with water and
101 THF in Fig. 2. The diffraction peaks can be ascribed to Mn₃O₄ in Fig. 2a. The other samples can also
102 be ascribed to Mn₃O₄ in Fig. 2b,c , respectively. All the Mn₃O₄ here are lack of the peak of (101),
103 which means that the is not the high-energy {101} plane.
104

105 The electrochemical performance of Mn_3O_4 nanoparticles and microflowers was evaluated as anode
106 materials for lithium-ion batteries (Fig. 3). Fig. 3a shows the 1st and 2nd charge–discharge profiles of
107 Mn_3O_4 microflowers at a current density of 240 mA g^{-1} (Sample T-72). A long discharge platform is
108 observed at 0.5 V in the first discharge curve, but this platform disappears in the succeeding
109 discharge curves. The Mn_3O_4 microflowers-based composite electrode delivers an initial discharge
110 capacity of 1496 mAh g^{-1} . However, the 1st discharge profiles of Mn_3O_4 nanoparticles show four
111 discharge platforms at 0.33, 0.44, 0.92 and 1.3V, implying that a multi-step conversion reaction takes
112 place. A new platform at 0.7 V appears in the succeeding discharge curves. The Mn_3O_4
113 nanoparticles-based composite electrode delivers an initial discharge capacity of 1280 mAh g^{-1} . It can
114 be seen that Mn_3O_4 without high-energy {101} plane can also have a very high initial discharge
115 capacity. It can also be found that Mn_3O_4 nanoparticles have a steeper charge curve than Mn_3O_4
116 microflowers between 1.4 and 3.0 V implying that a severe polarization takes place in the Mn_3O_4
117 nanoparticles-based composite electrode.

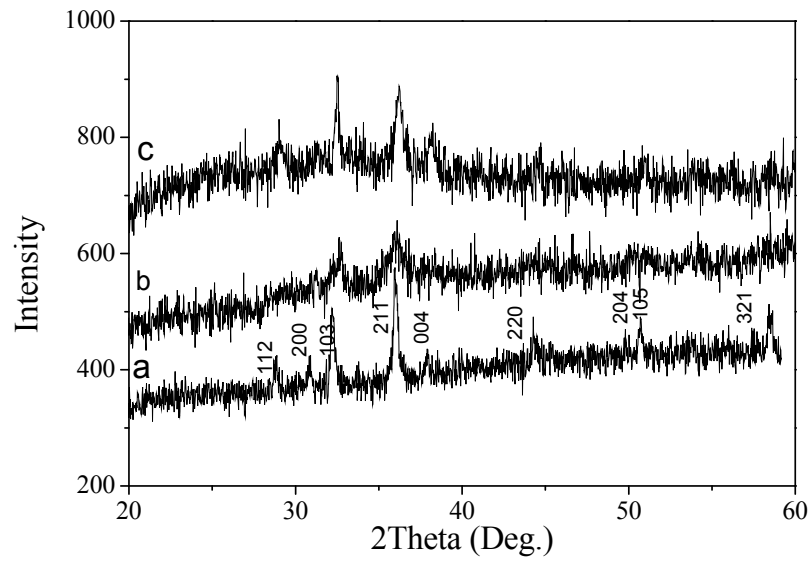
118
119 We also performed the $dQ/dV \sim V$ curves obtained from the 1st and 2nd charge-discharge curves of
120 Mn_3O_4 nanoparticles and microflowers in Fig. 4. In the first charge-discharge cycle of Mn_3O_4
121 nanoparticles, four reduction peaks are centered at 0.33, 0.45, 0.90 and 1.3 V, and the oxidation peak
122 is at 1.24 V in Fig. 4a. In the first charge-discharge cycle of Mn_3O_4 microflowers, the reduction and
123 oxidation peaks are centered at 0.33 and 1.28 V in Fig. 4b, respectively. In the second charge-
124 discharge cycle of Mn_3O_4 nanoparticles, two reduction peaks are centered at 0.45 and 0.52 V, and
125 the oxidation peak is at 1.24 V in Fig. 5b. In the second charge-discharge cycle of Mn_3O_4
126 microflowers, the reduction and oxidation peaks are centered at 0.54 and 1.25 V in Fig. 2,
127 respectively. The reduction peaks in the range of 1.3-0.4 V was ascribed to reduction from Mn(III) to
128 Mn(II), and the 0.4-0.1 V range reflected the reduction from Mn(II) to Mn(0) [47,48]. The difference of
129 first discharge curve between Mn_3O_4 microflowers and nanoparticles is because Mn_3O_4 microflowers
130 only undergoes the reduction from Mn(II) to Mn(0). While Mn_3O_4 nanoparticles undergo reductions
131 from Mn(III) to Mn(II) to Mn(0). In the second discharge process, In the second discharge, the
132 contribution to discharge capacity is mainly ascribed to the reduction around 0.5 V. The Li⁺ charge
133 reaction: is $\text{Mn}_3\text{O}_4 + 8\text{Li}^+ + 8\text{e}^- \rightarrow 3\text{Mn(0)} + 8\text{Li}_2\text{O}$ [49]. Compared to Mn_3O_4 nanoparticles, Mn_3O_4
134 microflowers does not undergo reduction from Mn(III) to Mn(II) and reduce polarization.

135
136 Fig.6 is the cycling performance testes at current densities of 240 and 480 mA g^{-1} . The Mn_3O_4
137 microflowers-based composite electrode delivers a second discharge capacity of 870.2 and 714.8
138 mAh g^{-1} in Fig. 6a,b, respectively . A reversible capacity of 392.8 and 358.5 mAh g^{-1} is retained after
139 20 cycles. The Mn_3O_4 nanoparticles-based composite electrode show lower discharge capacity and
140 worse cycling stability at current densities of 240 and 480 mA g^{-1} in Fig. 6c,d. It delivers a second
141 discharge capacity of 332.8 and 156.5 mAh g^{-1} , respectively. The final discharge capacity is even low
142 to 131.3 and 53.8 mA g^{-1} . The fast capacity decay of Mn_3O_4 nanoparticles is due to the reduction from
143 Mn(III) to Mn(II). The improved electrochemical performance of Mn_3O_4 microflowers is due to reduce
144 the activity of Mn_3O_4 , avoid the complicated reduction from Mn(III) to Mn(II) and reduce polarization.



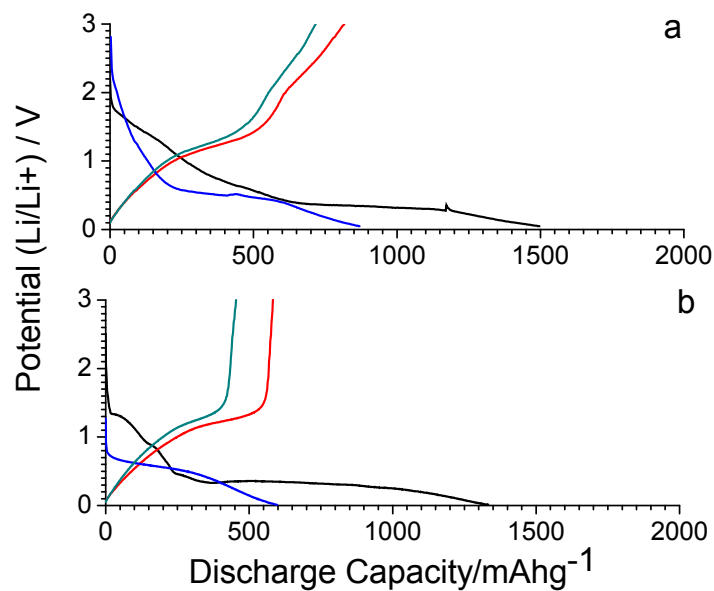
145
146
147
148

Fig. 1. SEM images of samples with (a, b) water, (c, d) water and DMF, and (e, f) water, DMF and CTABr



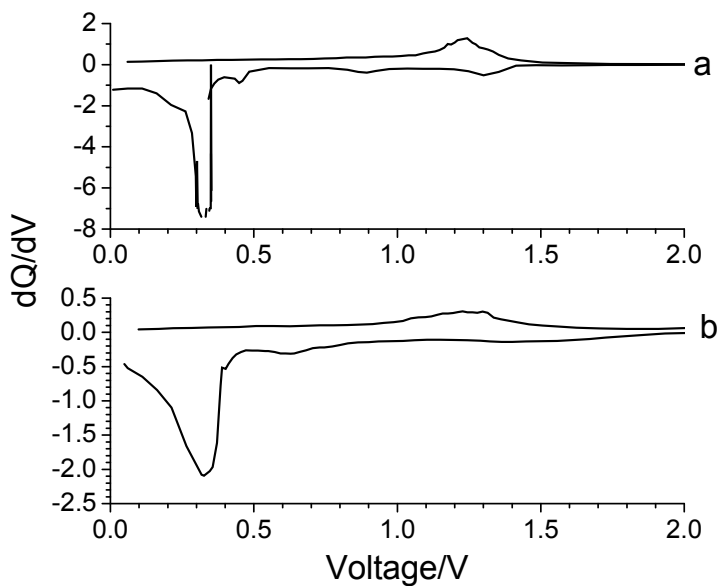
149
150
151
152

Fig. 2. Wide angle XRD patterns of samples with (a) water, DMF and CTABr, (b) water and DMF, and (c) water



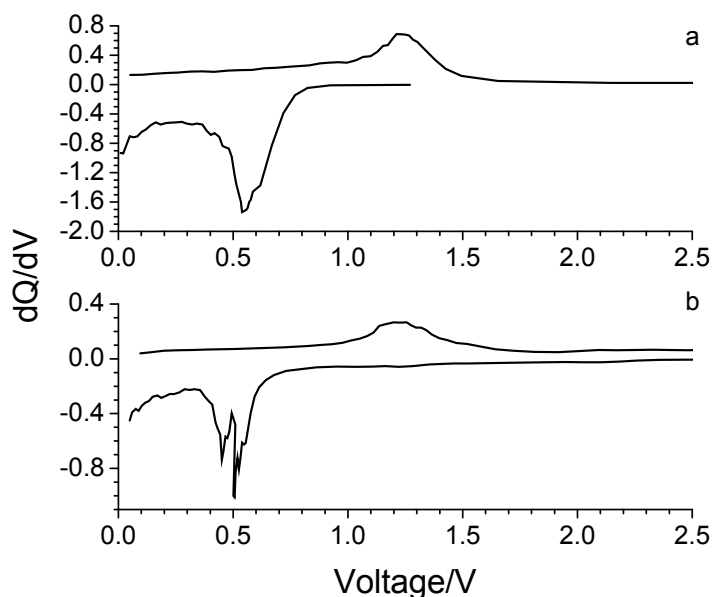
153
154
155
156
157

Fig. 3. The first and second charge–discharge profiles at a current density of 240 mA g^{-1} of (a) Mn_3O_4 microflowers and (b) Mn_3O_4 nanoparticles



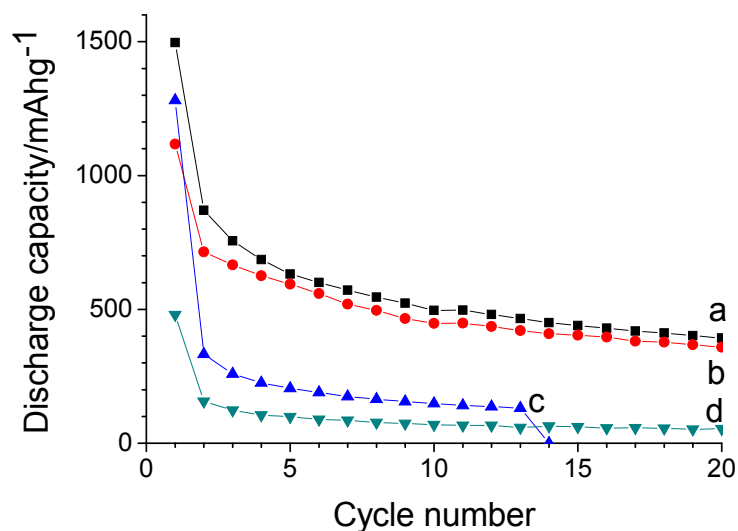
158
159
160
161

Fig. 4. The dQ/dV -curve derived the first charge–discharge profiles of (a) Mn_3O_4 nanoparticles (b) Mn_3O_4 microflowers



162
163
164
165
166

Fig. 5. The dQ/dV -curve derived the second charge–discharge profiles of (a) Mn_3O_4 microflowers (b) Mn_3O_4 nanoparticles



167
168
169
170
171
172
173
174
175
176
177
178
179

Fig. 6. The cyclic performance tested at current densities of 240 and 480 $mA g^{-1}$ of (a, b) Mn_3O_4 microflowers, and (c, d) Mn_3O_4 nanoparticles

4. CONCLUSION

In summary, Mn_3O_4 microflowers associated with super-thin nanosheets were prepared by using a solvo-thermal method with the aid of surfactant CTABr. The Mn_3O_4 microflowers exhibit better cycling stability and higher discharge capacity than Mn_3O_4 nanoparticles as anode materials for lithium-ion batteries due to reduce the activity of Mn_3O_4 , avoid the complicated reduction from Mn(III) to Mn(II) and reduce polarization. This simple method may also be used to fabricate other anode materials for lithium-ion batteries with improved electrochemical performance.

180
181
182
183
184
185
186
187
188
189
190
191
192
193
194
195
196
197
198
199
200
201
202
203
204
205
206
207
208
209
210
211
212
213
214
215
216
217
218
219
220
221
222
223
224
225
226
227
228
229
230
231
232
233
234
235
236
237
238

REFERENCES

1. Hilly M, Adams ML, Nelson SC. A study of digit fusion in the mouse embryo. *Clin Exp Allergy*. 2002;32(4):489-98. Cheng FY, Liang J, Tao ZL, Chen J. Functional materials for rechargeable batteries. *Adv Mater*. 2012;23:1695-1715.
2. Fei HL, Liu X, Li ZW. Hollow cobalt coordination polymer microspheres: a promising anode material for lithium-ion batteries with high performance. *Chem Eng J*. 2015;281:453-458.
3. Tarascon JM. Key challenges in future Li-battery research. *Phil. Trans. R. Soc. A.*, 2010;368:3227-3241.
4. Gao J, Lowe MA, Abruña HD, Spongelike nanosized Mn₃O₄ as a high-capacity anode material for rechargeable lithium batteries. *Chem Mater*. 2011;23:3223-3227.
5. Zhang LP, Li GS, Fan JM, Li BY. In situ synthesis of Mn₃O₄ nanoparticles on hollow carbon nanofiber as high-performance lithium ion battery anode. *Chem*. 2018;DOI:10.1002/chem.201801196.
6. Guo LG, Ding Y, Qin CQ et al, Anchoring Mn₃O₄ nanoparticles onto nitrogen-doped porous carbon spheres derived from carboxymethyl chitosan as superior anodes for lithium-ion batteries. *J Alloy Cmpd*. 2018;735:209-217.
7. Song NJ, Ma CL. A green synthesis of Mn₃O₄ /graphene nanocomposite as anode material for lithium-ion batteries. *Int J Electrochem Sci*. 2018;13:452-460.
8. Wu LL, Zhao DL, Cheng XW, Ding ZW, Hu T, Meng S. Nanorod Mn₃O₄ anchored on graphene nanosheet as anode of lithium ion batteries with enhanced reversible capacity and cyclic performance. *J Alloy Cmpd*. 2018;728:383-390.
9. Li Z, Tang B, Mn₃O₄/nitrogen-doped porous carbon fiber hybrids involving multiple covalent interactions and open voids as flexible anodes for lithium-ion batteries. *Green Chem*. 2017;19:5862-5873.
10. Liu BB, Qi L, Ye JJ, Wang JQ, Xu CX. Facile fabrication of graphene-encapsulated Mn₃O₄ octahedra cross-linked with a silver network as a high-capacity anode material for lithium ion batteries, *New J Chem*. 2017;41:13454-13461.
11. Peng HJ, Hao GX, Chu ZH, Lin J, Lin XM, Cai YP. Mesoporous Mn₃O₄/C microspheres fabricated from MOF template as advanced lithium-ion battery anode. *Crys Growth & Des*. 2017;11:5881-5886.
12. Lv KK, Zhang YH, Zhang DY, Ren WW, Sun L. Mn₃O₄ nanoparticles embedded in 3D reduced graphene oxide network as anode for high-performance lithium ion batteries. *J Mater Sci-Mater. El.*, 2017;28:14919-14927.
13. Pramanik A, Maiti S, Sreemany M, Mahanty S. Rock-salt-templated Mn₃O₄ nanoparticles encapsulated in a mesoporous 2D carbon matrix: a high rate 2 V anode for lithium-ion batteries with extraordinary cycling stability. *Chemistryselect*, 2017;2:854-7864.
14. Zhang R, Wang D, Qin LC, MnCO₃/ Mn₃O₄/reduced graphene oxide ternary anode materials for lithium-ion batteries: facile green synthesis and enhanced electrochemical performance. *J Mater Chem A*, 2017;5:17001-17011.
15. Zhuang YC, Ma Z, Deng YM, Song XN, Zuo XX, Xiao X, Nan JM. Sandwich-like Mn₃O₄/carbon nanofragment composites with a higher capacity than commercial graphite and hierarchical voltage plateaus for lithium ion batteries. *Electrochim Acta*. 2017;440-447.
16. Yang ZL, Lu DL, Zhao RR, Gao AM, Chen HY. Synthesis of a novel structured Mn₃O₄@C composite and its performance as anode for lithium ion battery. *Mater Lett*. 2017;198:97-100.
17. Cui X, Wang YQ, Xu QY, Sun P, Wang XZ, Wei T, Sun YM. Carbon nanotube entangled Mn₃O₄ octahedron as anode materials for lithium-ion batteries. *Nanotech*. 2017;28:255402.
18. Chen JY, Wu XF, Gong Y, Wang PF, Li WH, Tan QQ, Chen YF. Synthesis of Mn₃O₄/N-doped graphene hybrid and its improved electrochemical performance for lithium-ion batteries. *Ceram Int*. 2017;43:4655-4662.
19. Gangaraju D, Sridhar V, Lee I, Park H. Graphene - carbon nanotube - Mn₃O₄ mesoporous nanoalloys as high capacity anodes for lithium-ion batteries. *J Alloy Cmpd*. 2017;699:106-111.
20. Seong CY, Park SK, Bae Y, Yoo S, Piao Y. An acid-treated reduced graphene oxide/ Mn₃O₄ nanorod nanocomposite as an enhanced anode material for lithium ion batteries. *Rsc Adv*. 2017;7:37502-37507.
21. Park I, Kim T, Park H, Mun M, Shim SE, Baek SH. Preparation and electrochemical properties of Pt-Ru/ Mn₃O₄/C bifunctional catalysts for lithium-air secondary battery. *J Nanosci. Nanotechno*. 2016;16:10453-10458.

- 239 22. Zhang Y, Yue KQ, Zhao HS, Wu Y, Duan LF, Wang KL. Bovine serum albumin assisted synthesis
240 of Fe₃O₄@C@ Mn₃O₄multilayer core-shell porous spheres as anodes for lithium ion battery.
241 Chem Eng J. 2016;291:238-243.
- 242 23. Park SK, Seong CY, Yoo S, Piao Y. Porous Mn₃O₄ nanorod/reduced graphene oxide hybrid
243 paper as a flexible and binder-free anode material for lithium ion battery. Energy, 2016;99:266-
244 273.
- 245 24. Alfaruqi MH, Gim J, Kim S, Song J, Duong PT, Jo J, Baboo JP, Xiu Z, Mathew V, Kim J. One-step
246 pyro-synthesis of a nanostructured Mn₃O₄/C electrode with long cycle stability for rechargeable
247 lithium-ion batteries. Chem-A Eur J. 2016; 22:2039-2045.
- 248 25. Bhimanapati G, Yang RG, Robinson JA, Wang Q. Effect of Mn₃O₄ nanoparticle composition and
249 distribution on graphene as a potential hybrid anode material for lithium-ion batteries. Rsc Adv.
250 2016;6:33022-33030.
- 251 26. Jing MJ, Wang JF, Hou HS, Yang YC, Zhang Y, Pan CC, Chen J, Zhu YR, Ji XB. Carbon
252 quantum dot coated Mn₃O₄ with enhanced performances for lithium-ion batteries. J Mater Chem
253 A. 2015;3:16824-16830.
- 254 27. Ren YR, Wang JW, Huang XB, Yang B, Ding JN. One step hydrothermal synthesis of
255 Mn₃O₄/graphene composites with great electrochemical properties for lithium-ion batteries. Rsc
256 Adv. 2015;5:59208-59217.
- 257 28. Yue HW, Li F, Yang ZB, Li XW, Lin SM, He DY. Facile preparation of Mn₃O₄-coated carbon
258 nanofibers on copper foam as a high-capacity and long-life anode for lithium-ion batteries. J Mater
259 Chem A. 2014;2:17352-17358.
- 260 29. Luo S, Wu HC, Wu Y, Jiang KL, Wang JP, Fan SS. Mn₃O₄ nanoparticles anchored on
261 continuous carbon nanotube network as superior anodes for lithium ion batteries. J Power
262 Sources, 2014;249:463-469.
- 263 30. Park SK, Jin A, Yu SH, Ha J, Jang B, Bong S, Woo S, Sung YE, Piao Y. In situ hydrothermal
264 synthesis of Mn₃O₄ nanoparticles on nitrogen-doped graphene as high-performance anode
265 materials for lithium ion batteries. Electrochim Acta, 2014;120:452-459.
- 266 31. Luo YQ, Fan SS, Hao NY, Zhong SL, Liu WC. An ultrasound-assisted approach to synthesize
267 Mn₃O₄/RGO hybrids with high capability for lithium ion batteries. Dalton T. 2014;43:15317-15320.
- 268 32. Lavoie N, Malenfant PRL, Courtel FM, Abu-Lebdeh Y, Davidson IJ. High gravimetric capacity and
269 long cycle life in Mn₃O₄/graphene platelet/LiCMC compositelithium-ion battery anodes. J Power
270 Sources 2012;213:249-254.
- 271 33. Wang ZH, Yuan LX, Shao QG, Huang F, Huang YH. Mn₃O₄ nanocrystals anchored on multi-
272 walled carbon nanotubes as high-performance anode materials for lithium-ion batteries. Mater
273 Lett. 2012;80:110-113.
- 274 34. Wang CB, Yin LW, Xiang D, Qi YX. Uniform carbon layer coated Mn₃O₄ nanorod anodes with
275 improved reversible capacity and cyclic stability for lithium ion batteries. ACS Appl Mater Inter.
276 2012;4:1636-1642.
- 277 35. Li ZQ, Liu NN, Wang XK, Wang CB, Qi YX, Yin LW. Three-dimensional nanohybrids of
278 Mn₃O₄/ordered mesoporous carbons for high performance anode materials for lithium-ion
279 batteries. J Mater Chem. 2012;22:16640-16648.
- 280 36. Palaniandy N, Nkosi FP, Raju K, Ozoemena KI. Fluorinated Mn₃O₄ nanospheres for lithium-ion
281 batteries: Low-cost synthesis with enhanced capacity, cyclability and charge-transport. Mater
282 Chem Phys. 2018;209:65-75.
- 283 37. Jiang Z, Huang KH, Yang D, Wang S, Zhong H, Jiang CW. Facile preparation of Mn₃O₄ hollow
284 microspheres via reduction of pentachloropyridine and their performance in lithium-ion batteries.
285 RSC Adv. 2017;3:8264-8271.
- 286 38. Fan XY, Cui Y, Liu P, Gou L, Xu L, Li DL. Electrochemical construction of three-dimensional
287 porous Mn₃O₄ nanosheet arrays as an anode for the lithium ion battery. Phys Chem Chem Phys.
288 2016;18:22224-22234.
- 289 39. Zhen MM, Zhang Z, Ren QT, Liu L. Room-temperature synthesis of ultrathin Mn₃O₄ nanosheets
290 as anode materials for lithium-ion batteries. Mater Lett. 2016;177:21-24.
- 291 40. Li TT, Guo CL, Sun B, Li T, Li YG, Hou LF, Wei YH. Well-shaped Mn₃O₄ tetragonal bipyramids
292 with good performance for lithium ion batteries. J Mater Chem A. 2015;3:7248-7254.
- 293 41. Bai ZC, Zhang XY, Zhang YW, Guo CL, Tang B. Facile synthesis of mesoporous Mn₃O₄
294 nanorods as a promising anode material for high performance Lithium-ion batteries. J Mater Chem
295 A. 2014;2:16755-16760.
- 296 42. Huang SZ, Jin J, Cai Y, Li Y, Tan HY, Wang HE, Tendeloo GV, Su BL. Engineering single
297 crystalline Mn₃O₄ nano-octahedra with exposed highly active {011} facets for high performance
298 lithium ion batteries. Nanoscale, 2014;6 : 6819-6827.

- 299 43. Jian GQ, Xu YH, Lai LC, Wang CS, Zachariah MR. Mn₃O₄ hollow spheres for lithium-ion
300 batteries with high rate and capacity. *J Mater Chem A*. 2014;2:4627-4632.
- 301 44. Zhao DY, Hao Q, Xu CX, Facile fabrication of composited Mn₃O₄/Fe₃O₄ nanoflowers with high
302 electrochemical performance as anode material for lithium ion batteries. *Electrochim Acta*,
303 2015;180:493-500.
- 304 45. Wang JZ, Du N, Wu H, Zhang H, Yu JX, Yang DR, Order-aligned Mn₃O₄ nanostructures as
305 super high-rate electrodes for rechargeable lithium-ion batteries. *J. Power Sources*, 2013;222:32-
306 37.
- 307 46. Wang M, Cheng LM, Li QB, Chen ZW, Wang SL. Two-dimensional nanosheets associated with
308 one-dimensional single-crystalline nanorods self-assembled into three-dimensional flower-like
309 Mn₃O₄ hierarchical architectures. *Phys Chem Chem Phys*. 2014;39:21742-21746.
- 310 47. Pasero D, Reeves N, West AR, Co-doped Mn₃O₄: a possible anode material for lithium batteries.
311 *J Power Sources*. 2005;141:156-158.
- 312 48. Wang HL, Cui LF, Yang Y, Casalongue HS, Robinson JT, Liang YY, Cui Y, Dai HJ. Mn₃O₄-
313 graphene hybrid as a high-capacity anode material for lithium ion batteries. *J Am Chem Soc*.
314 2010;132:13978-13980.
- 315 49. Wu Z, Ren W, Wen L, Gao L, Zhao J, Chen Z, Zhou G, Li F, Cheng H. Graphene anchored with
316 Co₃O₄ nanoparticles as anode of lithium ion batteries with enhanced reversible capacity and
317 cyclic performance. *ACS Nano*, 2010;4:3187-3194.
- 318